PAPER

12- and 21-GHz Dual-Band Dual-Circularly Polarized Offset Parabolic Reflector Antenna Fed by Microstrip Antenna Arrays for Satellite Broadcasting Reception

Masafumi NAGASAKA[†a)], **Masaaki KOJIMA**[†], **Hisashi SUJIKAI**[†], ***Members***, ***and*** **Jiro HIROKAWA**[††], ***Fellow***

SUMMARY In December 2018, satellite broadcasting for 4K/8K ultra-high-definition television (UHDTV) will begin in Japan. It will be provided in the 12-GHz (11.7 to 12.75 GHz) band with right- and left-hand circular polarizations. BSAT-4a, a satellite used for broadcasting UHDTV, was successfully launched in September 2017. This satellite has not only 12-GHz-band right- and left-hand circular polarization transponders but also a 21-GHz-band experimental transponder. The 21-GHz (21.4 to 22.0 GHz) band has been allocated as the downlink for broadcasting satellite service in ITU-R Regions 1 (Europe, Africa) and 3 (Asia Pacific). To receive services provided over these two frequency bands and with dual-polarization, we implement and evaluated a dual-band and dual-circularly polarized parabolic reflector antenna fed by 12- and 21-GHz-band microstrip antenna arrays with a multilayer structure. The antenna is used to receive 12- and 21-GHz-band signals from in-orbit satellites. The measured and experimental results prove that the proposed antenna performs as a dual-polarized antenna in those two frequency bands and has sufficient performance to receive satellite broadcasts.

key words: *reflector antenna, microstrip antenna, circular polarization, dual band antenna, dual polarized antenna*

1. Introduction

4K/8K ultra-high-definition television (UHDTV) [1]–[3] will begin in Japan with the use of the latest broadcasting satellite, BSAT-4a, on December 1st, 2018. 2K high-definition television (HDTV) has been provided with right-hand circular polarization (RHCP) in the 12-GHz band (11.7 to 12.75 GHz) since 2000, and UHDTV satellite broadcasting will be additionally broadcasted with left-hand circular polarization (LHCP) in the same frequency band. The 21-GHz (21.4 to 22.0 GHz) band has also been allocated as the downlink for broadcasting satellite service in ITU-R Regions 1 (Europe, Africa) and 3 (Asia Pacific). To provide advanced services, such as 3DTV, onboard antennas and wide-bandwidth transponders for a 21-GHz-band broadcasting satellite have been studied [4]–[6].

BSAT-4a was successfully launched into its geostationary orbital position of 110 degrees East in September 2017. This satellite has not only 12-GHz-band RHCP and LHCP transponders but also a 21-GHz-band experimental transponder, which has 278 MHz bandwidth. A beacon signal in the 21-GHz band is also being transmitted from BSAT-4a continuously. The 21-GHz-band transponder will be used for various experiments, e.g., wideband-transmission and long term measurement of rain-attenuation. The 21-GHz band can be used, in addition to the 12-GHz band, to provided various satellite broadcasting services. However, installation of the receiving antennas corresponding to each frequency band requires a wider space and incurs higher costs. To solve these problems, a 12- and 21-GHz dual-band dual-circularly polarized reflector antenna will be required that can receive the broadcasting services provided over these two different frequency bands and with dual-polarization.

For satellite broadcasting reception, various types of antennas have been studied. For example, a radial line slot antenna (RLSA) [7], helical array antenna [8], microstrip array antenna [9], and leaky waveguide array antenna [10] have been reported. These antennas were designed to receive signals transmitted with RHCP in the 12-GHz band. A dual-circularly polarized RLSA [11] has also been reported. This RLSA was designed in accordance with the specifications for satellite broadcasting in the United States at the time (12.2 to 12.7 GHz), whose frequency bandwidth was half that of the 12-GHz band (11.7 to 12.75 GHz).

Because the costs of producing parabolic reflector antennas are lower than those of array antennas, offset parabolic reflector antennas are generally used. Septum polarizers have been reported for a polarizer of dual-circularly polarized reflector antennas [12]–[14]. They provide good circularity and require no adjustments. However, it is difficult to share a septum polarizer with the 12- and 21-GHz bands because we have to decide its design parameters in accordance with each frequency band. A horn antenna is connected to the septum polarizer, and the aperture diameter suitable for the 12- and 21-GHz band is also different. We cannot set two horn antennas, for each frequency band, at the focal point of a parabolic reflector. Therefore, it is impossible for a conventional receiving antenna to capture 12- and 21-GHz band signals with dual polarizations (LHCP and RHCP) simultaneously.

For receiving Ku- and Ka- bands, a reflectarray antenna is reported [15]. This antenna has a frequency-selective surface and can receive 12.25 to 12.75 GHz and 19.6 to 21.2 GHz simultaneously. However, the receiving polar-

Manuscript received September 11, 2018.
Manuscript revised November 29, 2018.
Manuscript publicized January 9, 2019.

[†]The authors are with NHK Science & Technology Research Laboratories, Japan Broadcasting Corporation, Tokyo, 157-8510 Japan.
[††]The author is with Department of Electrical and Electronic Engineering, Tokyo Institute of Technology, Tokyo, 152-8552 Japan.
a) E-mail: nagasaka.m-hm@nhk.or.jp

DOI: 10.1587/transcom.2018EBP3257

izations of Ku- and Ka- bands are linear polarization and LHCP, respectively. For circularly polarized antennas in dual-frequency bands, various microstrip antennas (MSAs) have been studied [16]–[18]. We can obtain enough gain for satellite communications by configuring an array antenna with MSAs. However, grating lobes will appear in the 21-GHz band when the spacing of elements is more than one wavelength (λ) in the 21-GHz band, which is equivalent to 0.56 λ in the 12-GHz band. This is a restriction on the design of array antennas using dual-band MSAs.

Therefore, we proposed and have studied a dual-circularly polarized offset parabolic reflector antenna fed by 12- and 21-GHz-band MSA arrays with a multilayer structure for receiving services provided in those frequency bands [19], [20]. This proposed antenna is the result of our progress of the previous paper [21] in which we reported a 12-GHz-band dual-circularly polarized parabolic reflector antenna with an MSA array. In this paper, we have improved the feed antenna (MSA array) to be able to receive the 12- and 21-GHz bands simultaneously by designing a 21-GHz-band MSA, a dual-band feed circuit, and the multilayer structure. Previously, a dual-band reflector antenna that has a feed antenna composed of a horn antenna and an MSA array was reported [22]. The horn antenna and MSA array were set at the focal point of the offset parabolic reflector; however, the ratio of the upper to lower frequency-band had to be more than 5 to adopt the technique in the report.

In this paper, we describe a detailed design of a 12- and 21-GHz dual-band dual-circularly polarized offset parabolic reflector antenna fed by MSA arrays, and we present the measured results of a prototype antenna. To obtain enough gain and cross-polarization discrimination (XPD) throughout both bands for satellite broadcasting reception, the feed antenna is composed of two 2×2 MSA arrays that are sequentially rotated to enhance polarization purity [23]. In Sect. 2, we discuss the design of our proposed antenna and report on the measured performance in Sect. 3. In Sect. 4, we show an experiment on receiving 12- and 21-GHz-band signals from broadcasting satellites with our fabricated antenna. Finally, we conclude in Sect. 5.

2. Design of 12- and 21-GHz Dual-Band Dual-Circularly Polarized Receiving Reflector Antenna for Satellite Broadcasting

2.1 Performance Targets and Basic Configuration of Receiving Reflector Antenna

The performance targets for the 12- and 21-GHz dual-band dual-circularly polarized receiving reflector antenna are listed in Table 1. The gain values in the 12- and 21-GHz bands were 33 and 38 dBi, respectively, which were determined from the peak gain of a 45-cm parabolic reflector antenna (aperture efficiency: 60%). The XPD was derived from the reference pattern in Recommendation ITU-R BO.1213 [24] at boresight. The upper limit of the voltage standing wave ratio (VSWR) was 1.5 throughout the 12- and 21-GHz bands to enable small signals to be received from the satellite.

Table 1 Performance targets for receiving reflector antenna.

Frequency bands	12-GHz band	21-GHz band
Receiving frequencies	11.7 to 12.75 GHz	21.4 to 22.0 GHz
Polarizations	RHCP and LHCP	RHCP and LHCP
Gain	33 dBi	38 dBi
XPD	$\geq$ 25 dB (at boresight)	$\geq$ 25 dB (at boresight)
VSWR	$\leq$ 1.5	$\leq$ 1.5
Impedance	50 Ω	50 Ω

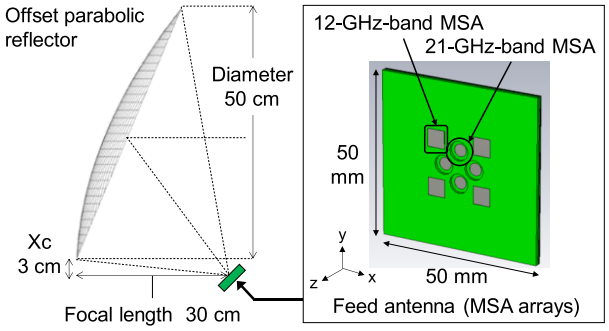

Fig. 1 Configuration of proposed antenna.

The configuration of our proposed reflector antenna is shown in Fig. 1. We selected an offset parabolic reflector generally used for satellite receiving antennas. The reflector is fed by 12- and 21-GHz-band MSA arrays located on the same focal point with a multilayer structure. This feed antenna uses two 2 × 2 MSA arrays to obtain a suitable beamwidth for each band. We assumed that the size of the feed antenna was 50×50 mm, which is equivalent to that of a low-noise block converter with a horn antenna for consumer use in Japan. Therefore, to avoid blocking receiving signals, we determined the clearance (Xc in Fig. 1) of the reflector to be 3 cm. A 50-cm-diameter reflector was selected to obtain enough gain in both bands assuming feeding loss in the MSA arrays. To mitigate a beam squint angle [25], the focal length is 30 cm, i.e., the ratio of the focal length to the diameter (F/D) is 0.6. In this study, we manufactured and tested a 12- and 21-GHz-band dual-circularly polarized parabolic reflector antenna fed by the MSA arrays.

2.2 Design of Dual-Circularly Polarized Wide-Band Microstrip Antenna

Figures 2 and 3 show the configuration of the 12- and 21-GHz-band MSAs we designed. Each MSA has an open stub for impedance matching, which enables us to adjust the impedance of the MSAs widely. To obtain a wide frequency bandwidth in the 12-GHz band (11.7 to 12.75 GHz), which is 1050 MHz, i.e., the fractional bandwidth is 8.6%, the MSAs have a multilayer structure that uses polytetrafluoroethylene (PTFE) substrates (ε_r is 2.55, and tan δ is 0.0015,

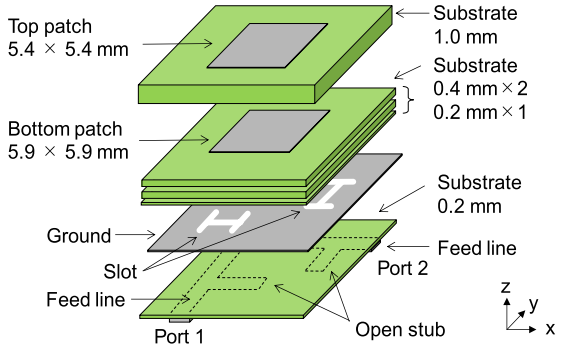

Fig. 2 Designed 12-GHz-band MSA.

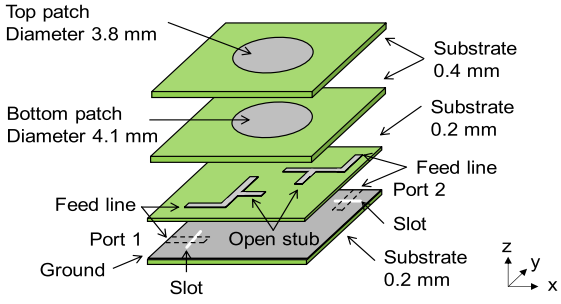

Fig. 3 Designed 21-GHz-band MSA.

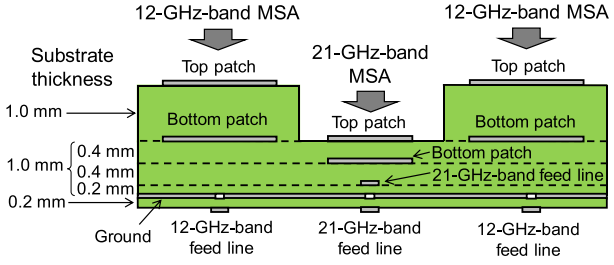

Fig. 4 Layer configuration of MSAs (schematic).

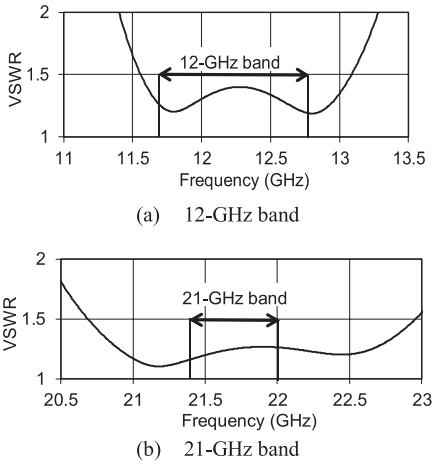

Fig. 5 Calculated VSWR of designed MSAs.

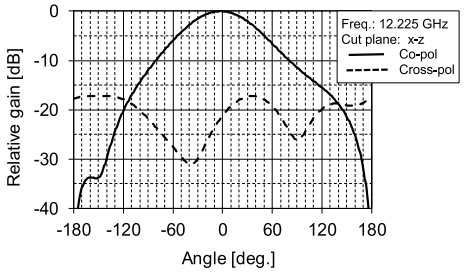

Fig. 6 Calculated radiation pattern of 12-GHz-band MSA.

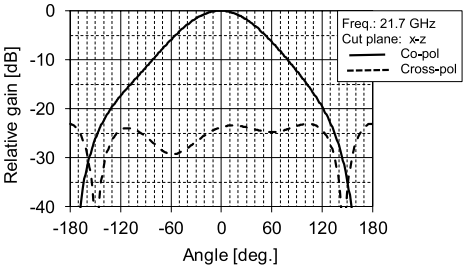

Fig. 7 Calculated radiation pattern of 21-GHz-band MSA.

typically). We used a stacked structure for the MSAs to obtain enough frequency bandwidth, especially in the 12-GHz band. We also used this structure for the 21-GHz band to avoid mismatching due to frequency-shifting by fabrication error. We can increase the impedance bandwidth with a thick substrate, but there is a physical limit to the substrate thickness. Hence, the maximum substrate thickness was set to $\lambda\varepsilon/16$ [26], where $\lambda\varepsilon$ is the wavelength in the dielectric. We arranged three substrates between the ground plane and the 12-GHz-band bottom patch, as shown in Fig. 4, since the maximum thickness in the 21-GHz band is smaller than that in the 12-GHz band.

The MSAs have two feeding ports to obtain circular polarization. For the 12-GHz-band MSA, feeding is realized by electromagnetic coupling with the bottom patch via feeding slots. For the 21-GHz band, we arranged the 21-GHz-band feed lines above the ground plane and coupled them onto the feed circuit with slots because a dual-band feed circuit became complicated. Then, feeding is realized by proximity coupling with the bottom patch for the 21-GHz band. The coupling slot on the ground plane for the 21-GHz band has a width of 0.1 mm and a length of 4.6 mm, and the calculated VSWR and insertion loss of the slot were not more than 1.14 and 0.5 dB throughout the 21-GHz band, respectively. In the following sections, we used a 3D electromagnetic field analysis simulator, CST MW Studio [27], to analyze the antenna characteristics of the MSAs and MSA arrays. Figure 5 shows the calculated VSWRs of the MSAs. We confirmed that the VSWR was within our target throughout both bands. The maximum values of the 12- and 21-GHz bands were 1.4 and 1.3, respectively.

The circular polarization was provided by feeding 90-deg.-shifted signals to the two feed lines. When the feeding phase of port 2 was delayed for 90 deg., the MSAs radiated RHCP, and when the feeding phase of port 1 was delayed for 90 deg., the MSAs radiated LHCP. Figures 6 and 7 show the calculated radiation patterns of the MSAs. The solid

and dashed lines show co-polarization (co-pol) and cross-polarization (cross-pol) patterns, respectively. The calculated frequencies were 12.225 and 21.7 GHz (the center frequency of each band). From these radiation patterns, we can see that the designed MSAs operate as circular polarized antennas.

However, the beamwidth of the co-pol patterns was too broad to use for the feed antenna of the offset parabolic reflector antenna. The XPDs (at 0 deg.) were also less than 25 dB, which is our target. The radiation pattern of the 12-GHz band MSA was asymmetric because the coupling slots were not in the center of the patch. It is difficult to obtain a narrower beamwidth with a single MSA, and we cannot set the coupling slots in the center of the 12-GHz-band MSA because its size is small. Therefore, we designed a 2×2 MSA array for each band to obtain a narrower beamwidth and applied a sequentially rotated array technique [23] for the array to improve the XPD.

2.3 Design of Dual-Band and Dual-Circularly Polarized Feed Antenna with Microstrip Antenna Arrays

Figures 8–10 show the configuration and feed circuit of our designed feed antenna using the MSAs described in the previous subsection. This antenna was composed of two 2×2 MSA arrays in which the elements were sequentially rotated to enhance the polarization purity [23]. We arranged the 21-GHz-band feed lines above the ground plane and coupled them onto the feed circuit with slots, which are at the eight points shown in Fig. 9, to configure a 12- and 21-GHz-band feed circuit on the substrate. The slot coupling was selected to avoid cost increases because of via holes under the assumption of mass production. Our designed feed circuit can output 12- and 21-GHz-band dual-polarized signals into the four ports shown in Fig. 10. The polarizations, which are discussed in this section, are defined as the polarizations radiated from the feed antenna.

The feeding phases in the 12- and 21-GHz bands are shown in Figs. 11 and 12, respectively. The feeding phase of the m−th patch is shifted to $90 \times (m - 1)$ deg. by using 3-dB, 90-deg. hybrid couplers (3dB-HYBs) and differences in the line length. Because the MSAs are fed two 90-deg.-shifted signals, the feeding phases of the adjacent MSA are

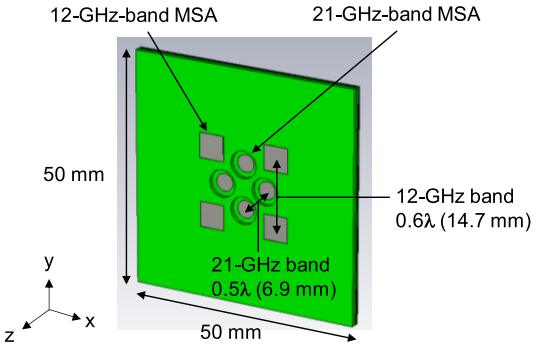

Fig. 8 Top view of designed feed antenna (MSA arrays).

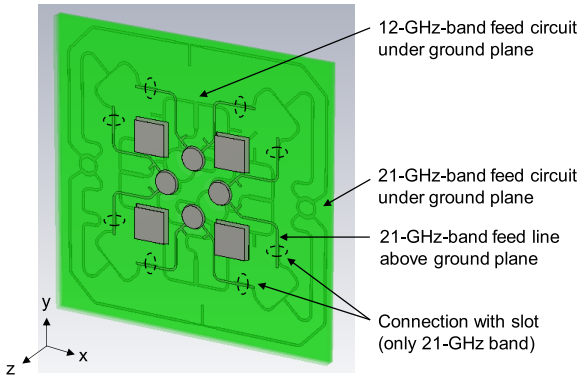

Fig. 9 Perspective view of designed feed antenna.

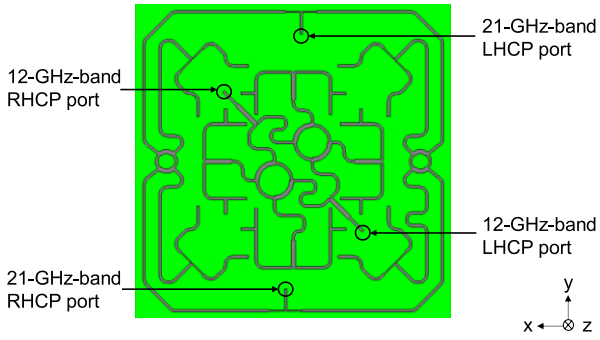

Fig. 10 Feed circuit (back view).

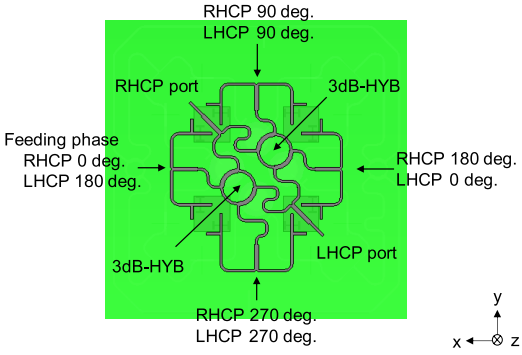

Fig. 11 Feeding phase in 12-GHz band (perspective view).

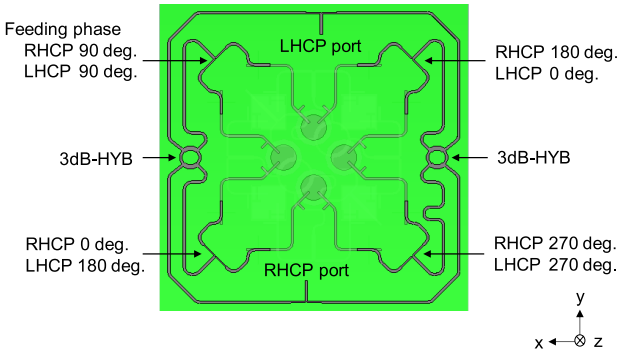

Fig. 12 Feeding phase in 21-GHz band (perspective view).

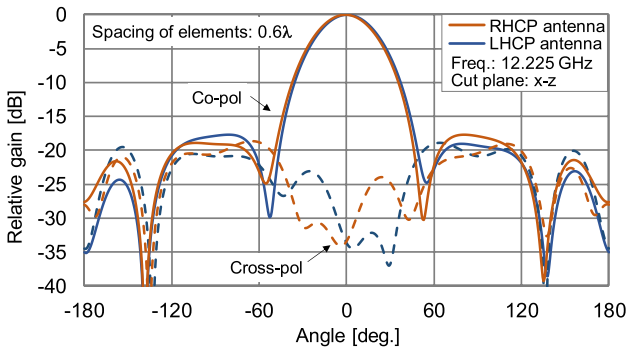

(a) 12-GHz band

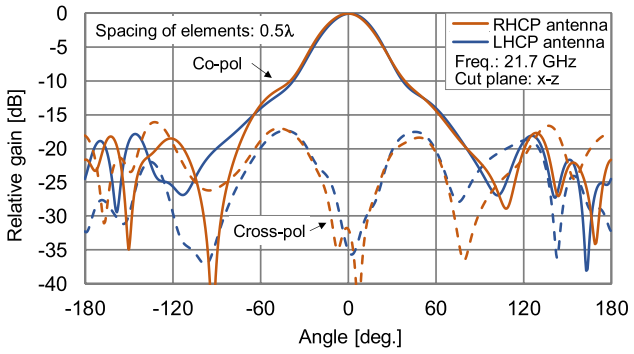

(b) 21-GHz band

Fig. 13 Calculated radiation patterns of feed antenna (MSA arrays).

made the same by applying the sequential rotation technique. Therefore, there are no cross sections of the feeding lines in our designed circuit except for the 21-GHz-band feed lines above the ground plane.

We optimized the spacing of elements to obtain a higher gain for each band, respectively. As shown in Fig. 1, the F/D of our designed reflector was 0.6, and our target edge illumination level (EIL) was −11 dB [28] at 39 deg. for both 12- and 21-GHz bands. The calculated radiation patterns of the feed antenna are shown in Fig. 13. The solid and dashed lines show the co- and cross-pol patterns, respectively. In the 12-GHz band, we selected 0.6 λ for the spacing of elements, and the calculated EILs of the RHCP and LHCP were −11.7 and −11.8 dB, respectively. Moreover, the XPD was more than 30 dB, which achieved our target value (25 dB), and the axial ratio of the RHCP and LHCP were 0.37 and 0.36 dB, respectively.

For the 21-GHz band, the radiation patterns were distorted because of unwanted emissions, as shown in Fig. 13(b). The emissions were radiated from the 21-GHz-band feed lines above the ground plane. Therefore, we studied EILs in the 21-GHz-band so that the reflector antenna's gain became peak. In this study, we calculated the radiation patterns of the feed antenna by changing the spacing of elements in the 21-GHz band. Then, the gains of the reflector antenna were obtained from the feed antenna's radiation patterns. We used reflector antenna analysis software, GRASP [29], to calculate the gain.

Table 2 Calculated gain of reflector configuration (without feeding loss).

Frequency [GHz]	Spacing of elements [λ]	EIL [dB]		Gain [dBi]		Selection
		RHCP	LHCP	RHCP	LHCP	
12.225	0.600	−11.7	−11.8	34.5	34.6	✓
21.7	0.475	−9.8	−10.2	38.2	38.2	
21.7	0.500	−9.9	−10.4	38.2	38.3	✓
21.7	0.525	−10.4	−10.8	38.2	38.2	
21.7	0.550	−10.4	−10.9	38.2	38.2	
21.7	0.600	−11.1	−11.6	37.8	37.9	
21.7	0.650	−12.3	−12.8	37.3	37.3	

Table 2 shows the calculated gain, which does not include the feeding loss. From this result, we decided the spacing to be 0.5 λ in the 21-GHz band because the highest gain was obtained. The EILs of the RHCP and LHCP were −9.9 and −10.4 dB, respectively. Moreover, the XPD was more than 30 dB, and the axial ratios of the RHCP and LHCP were 0.44 and 0.31 dB, respectively.

3. Prototype of 12- and 21-GHz Dual-Band Dual-Circularly Polarized Parabolic Reflector Antenna

3.1 Prototype Antenna

We fabricated and tested our 12- and 21-GHz dual-band dual-circularly polarized offset parabolic reflector antenna we designed. Figure 14 shows the prototype antenna. The reflector was fabricated by machining an aluminum panel to evaluate the radiation patterns of the reflector accurately. Reflectors made with pressed aluminum are generally for consumer use. We estimated that the gain degradation in the 12- and 21-GHz-bands due to reflector error [30] was 0.1 and 0.2 dB, respectively. The error of a reflector made with pressed aluminum was 0.26 mm RMS on the basis of our measurement results [31].

Figure 15 shows our fabricated feed antenna composed of two 2×2 MSA arrays. The antenna has four SMP connectors to connect the coaxial cables for our measurements. The substrates, of which our multilayer structure is configured, are fixed with plastic screws, and we did not use prepregs for attaching the substrates. A photograph of each substrate is shown in Fig. 16. The size of the substrate is 65 × 65 mm to make space for the screw holes. The ground plane is smaller than the substrate, as shown in the 5th layer substrate of Fig. 16. The size is 50 × 50 mm and equals to the initial design shown in Fig. 8. The copper thickness of the 5th layer is 35 μm, and that of the other layers is 18 μm.

We have studied the relationship of the mutual coupling and spacing of elements for a 12- and 21-GHz dual-band MSA array [32] and evaluated the measured radiation patterns of a dual-band feed (MSA array) that we previously fabricated [33]. On the basis of this knowledge, we designed and tested the 12- and 21-GHz dual-band dual-circularly polarized receiving reflector antenna in order to comprehensively evaluate it in this work.

Fig. 14 Fabricated receiving reflector antenna.

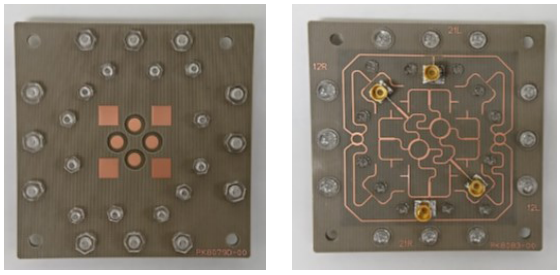

(a) Front view (b) Back view

Fig. 15 Fabricated feed antenna composed of MSA arrays.

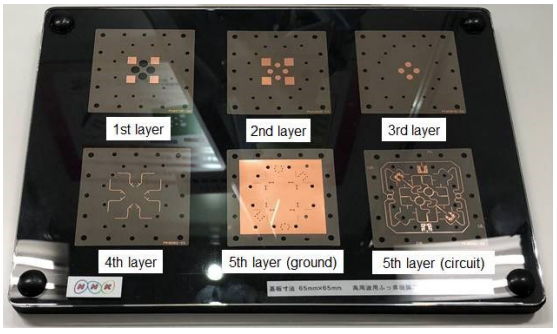

Fig. 16 Substrates composing feed antenna we fabricated.

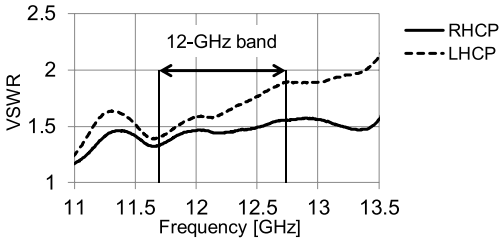

Fig. 17 Measured VSWR in 12-GHz band.

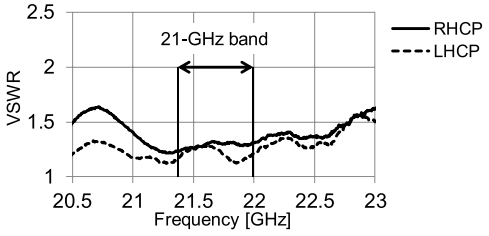

Fig. 18 Measured VSWR in 21-GHz band.

Table 3 Gain, aperture efficiency, and XPD of fabricated receiving antenna in 12-GHz band (include feeding loss).

Frequency [GHz]	Gain [dBi]	Aperture efficiency [%]	XPD [dB] (at boresight)
11.7	RHCP: 33.5 LHCP: 33.7	RHCP: 59.3 LHCP: 62.0	RHCP: 24.3 LHCP: 23.7
12.225	RHCP: 34.1 LHCP: 33.6	RHCP: 62.7 LHCP: 55.7	RHCP: 28.0 LHCP: 30.7
12.75	RHCP: 33.8 LHCP: 33.2	RHCP: 53.5 LHCP: 46.6	RHCP: 21.3 LHCP: 21.5

Table 4 Gain, aperture efficiency, and XPD of fabricated receiving antenna in 21-GHz band (include feeding loss).

Frequency [GHz]	Gain [dBi]	Aperture efficiency [%]	XPD [dB] (at boresight)
21.4	RHCP: 36.3 LHCP: 36.7	RHCP: 33.9 LHCP: 37.1	RHCP: 25.8 LHCP: 23.1
21.7	RHCP: 35.9 LHCP: 36.8	RHCP: 30.1 LHCP: 36.7	RHCP: 23.4 LHCP: 20.2
22.0	RHCP: 36.0 LHCP: 36.7	RHCP: 30.0 LHCP: 35.3	RHCP: 25.6 LHCP: 29.6

3.2 VSWR

Figures 17 and 18 show the measured VSWRs of the fabricated antenna. We measured the VSWRs with the feed antenna, which was installed on the reflector as shown in Fig. 14. The polarizations, which are discussed in this section, are defined as the polarizations radiated from the parabolic reflector antenna. We can see that this antenna covered the 12- and 21-GHz bands with VSWRs of 1.9 and 1.3, respectively. The measured values in the 21-GHz band met our performance target (VSWR of 1.5), but that in the 12-GHz band slightly exceeded the target. It is assumed that the degradation in VSWR was caused by variations in the substrate thickness.

3.3 Gain, Aperture Efficiency, and XPD

The measured gain, aperture efficiency, and XPD in the 12- and 21-GHz bands are listed in Tables 3 and 4, respectively. The gain was obtained by comparing a standard gain horn antenna and the fabricated antenna. We evaluated them in the lower-end, center, and upper-end frequencies of both bands. The measured values include the feeding loss. We can see that the deviation of the frequency response in the gain was less than 1 dB, and the XPD was more the 20 dB in the 12- and 21-GHz bands for both polarizations. These

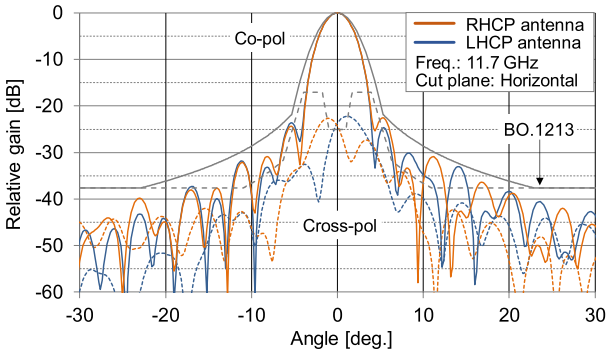

(a) Lower-end frequency (11.7 GHz)

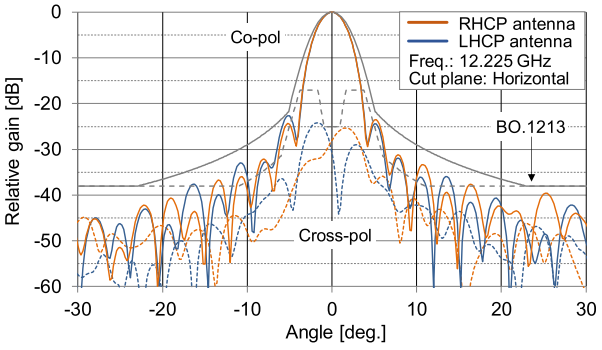

(b) Center frequency (12.225 GHz)

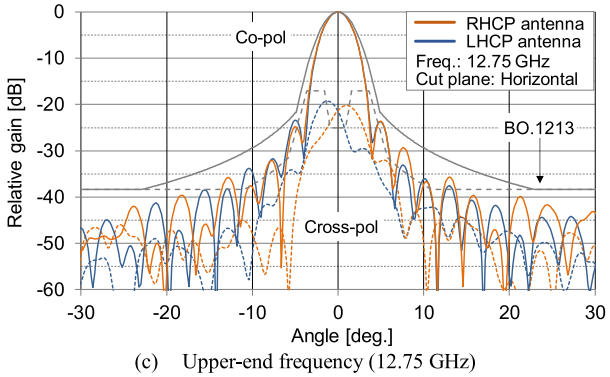

(c) Upper-end frequency (12.75 GHz)

Fig. 19 Radiation patterns of fabricated antenna in 12-GHz band.

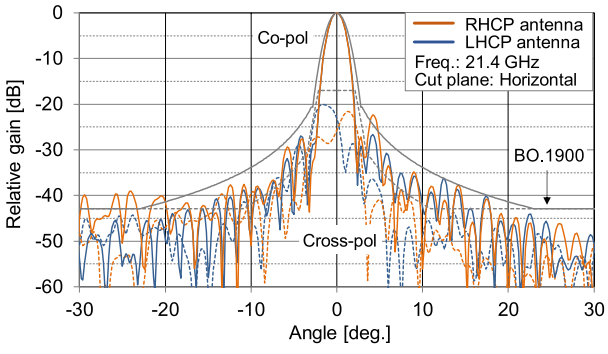

(a) Lower-end frequency (21.4 GHz)

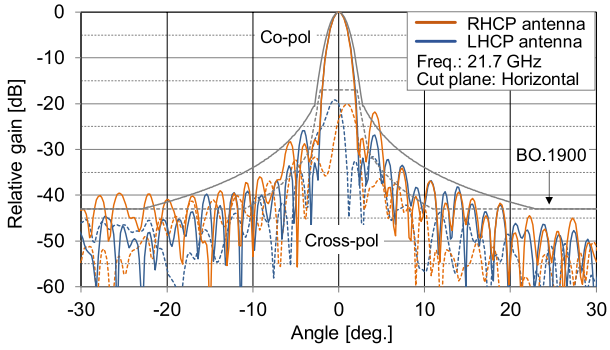

(b) Center frequency (21.7 GHz)

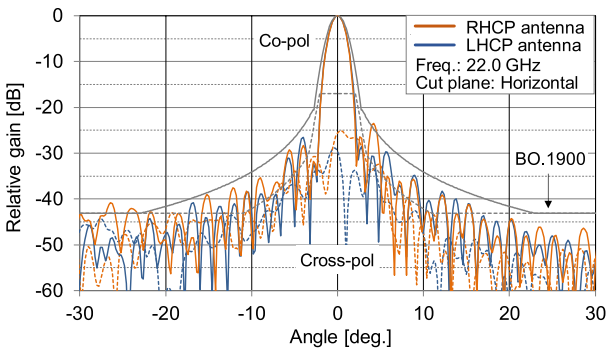

(c) Upper-end frequency (22.0 GHz)

Fig. 20 Radiation patterns of fabricated antenna in 21-GHz band.

results indicate that the fabricated antenna performed as a dual-circularly polarized antenna in both bands.

The measured gain met our target (33 dBi) in the 12-GHz band but was lower than that of the target (38 dBi) in the 21-GHz band. Our targets for the gain correspond to the aperture efficiency of 50% (at the center frequency) for the 50-cm-diameter reflector we used. The gains at each center frequency in the 12- and 21-GHz bands were about 34 and 36 dBi, respectively. Comparing these gains and the calculated values (Table 2), we found that it is necessary to reduce the feeding loss, especially in the 21-GHz band. The measured XPDs were also lower than that of our target (25 dB) because the feeding phase was shifted with the dimension error in the lines and 3-dB hybrid couplers.

3.4 Radiation Patterns

We measured the radiation patterns of the fabricated reflector antenna by using a spherical near-field antenna measurement system [34] in an acoustic chamber. The measured frequencies were the lower-end, center, and upper-end frequencies of the 12- and 21-GHz bands, which were 11.7, 12.225, 12.75, 21.4, 21.7, and 22.0 GHz. We evaluated the horizontal plane, which corresponds to geostationary orbit.

Figures 19 and 20 show the measured radiation patterns of the fabricated reflector antenna. The solid and dashed lines indicate co- and cross-polarization patterns, respectively. These figures also show the reference radiation patterns recommended by ITU-R for receiving earth station antennas. Rec. ITU-R BO.1213 (BO.1213) [24] is a refer-

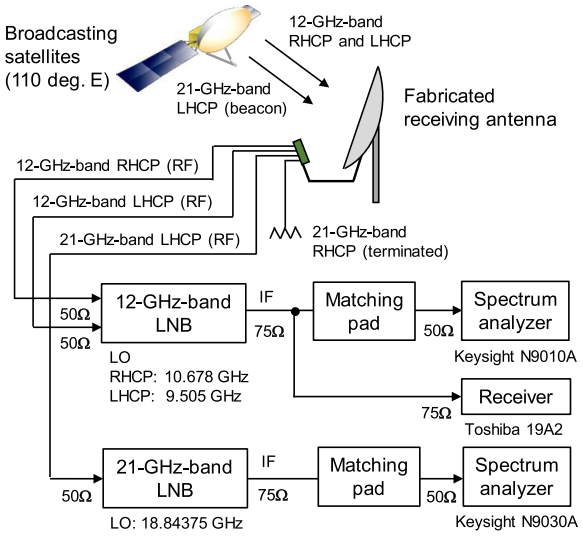

Fig. 21 Configuration of our experiment.

Table 5 Specifications of LNBs used for our experiment.

	12-GHz-band LNB	21-GHz-band LNB
Receiving freq. [GHz]	11.7 to 12.75	21.4 to 22.0
Local oscillator freq. [GHz]	RHCP: 10.678 LHCP: 9.505	18.84375
Gain [dB]	RHCP: 52 to 55 LHCP: 51 to 54	57 to 59
Noise figure [dB]	1.3 (typ.)	1.5 (typ.)
Output freq. [GHz]	RHCP: 1.03 to 2.07 LHCP: 2.22 to 3.22	2.55 to 3.16

ence pattern for the 12-GHz band, and Rec. ITU-R BO.1900 (BO.1900) [35] is that for the 21-GHz band. We compared the measured radiation patterns with the reference patterns because BO.1213 and BO.1900 are used for calculating interference in the coordination of satellite networks. We can see that the radiation patterns mostly satisfied the reference patterns.

4. Experiment on Receiving 12- and 21-GHz-Band Signals from Broadcasting Satellites with Prototype Receiving Antenna

4.1 Configuration of Experiment

We received the 12- and 21-GHz-band signals transmitted from broadcasting satellites with our prototype receiving antenna. The configuration of the experiment is shown in Fig. 21. The 12-GHz-band signals are transmitted from the BSAT [36] and JCSAT [37] satellites whose orbital positions are 110 deg. E. In the 21-GHz band, we can receive an LHCP signal that is the beacon (continuous wave) transmitted by BSAT-4a. We can receive an RHCP signal in the 21-GHz band only when an experimental signal is being transmitted from the transponder because there is no commercial broadcast service in the 21-GHz band yet [38].

Since the receiving power from the satellites is low, we connected low-noise block converters (LNBs) to the output of the receiving antenna. Therefore, we confirmed the presence of the receiving signals in the intermediate frequency (IF) bands. The specifications of the LNBs are listed in Table 5 and were customized for this experiment. The local oscillator frequency (LO) for the 12-GHz-band com-

(a) Fabricated antenna receiving signals from satellites

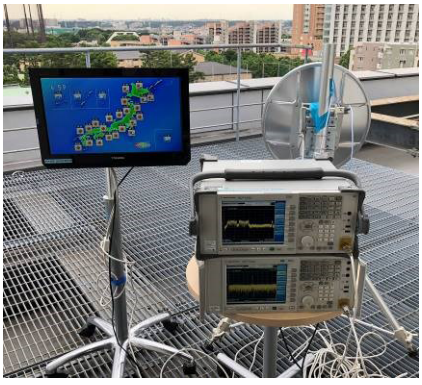

(b) Receiver and spectrum analyzers

Fig. 22 Experiment performed on June 1st, 2018.

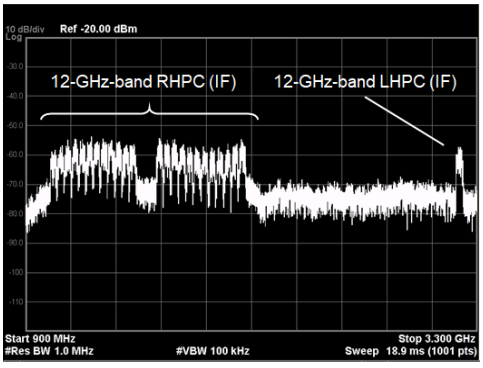

Fig. 23 Received spectrum of 12-GHz-band satellite broadcasting.

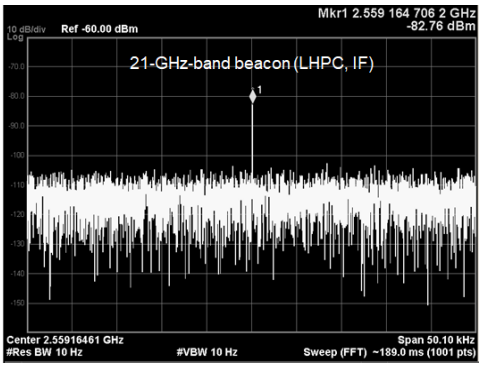

Fig. 24 Received spectrum of 21-GHz-band beacon.

plies with ARIB STD-B63 [39], which is a standard for 4K/8K UHDTV satellite broadcasting receivers in Japan, and that for the 21-GHz-band was chosen to correspond with a wide-band demodulator [40]. When we performed the experiment, 4K/8K UHDTV receivers were not available yet, and the 21-GHz-band wide-band modulated signal was not transmitted; therefore, we used spectrum analyzers and a consumer HDTV receiver for satellite broadcasting to verify the received signals.

4.2 Experimental Results

Our experiment was performed at NHK Science & Technology Research Laboratories (Setagaya, Tokyo) on June 1st, 2018. Pictures of the experiment are shown in Fig. 22. The BSAT and JCSAT satellites were transmitting signals from 24 transponders for RHCP and from one transponder for LHCP in the 12-GHz band on that day. BSAT-4a was also transmitting the beacon with the LHCP signal in the 21-GHz band; however, the experimental signal with RHCP was not transmitting in the band.

The frequency spectrums of the received signals are shown in Figs. 23 and 24. In Fig. 23, we can see that the RHCP and LHCP signals in the 12-GHz band were received simultaneously. For the 21-GHz band, the beacon signal was received adequately, as shown in Fig. 24. We also demodulated the 12-GHz-band receiving signal with the consumer satellite broadcasting receiver. The demodulated video and audio were totally normal. From the results, we confirmed that our developed antenna could receive the dual-circular polarizations in the 12-GHz band and the LHCP in the 21-GHz band simultaneously.

5. Conclusion

We manufactured and evaluated a dual-band and dual-circularly polarized offset parabolic reflector antenna for satellite broadcast reception in the 12-GHz (11.7 to 12.75 GHz) and 21-GHz (21.4 to 22.0 GHz) bands. The antenna is composed of a 50-cm offset parabolic reflector fed by 12- and 21-GHz-band MSA arrays with a multilayer structure. Measured results indicate that the antenna gains in the 12- and 21-GHz bands were about 34 and 36 dBi (aperture efficiencies were about 60 and 30%) at each center frequency, respectively. The VSWR was less than 1.9, and the XPD was more than 20 dB throughout both bands. We also received 12- and 21-GHz-band signals from broadcasting satellites with the prototype antenna simultaneously. We confirmed that our proposed antenna performed as a dual-circularly polarized antenna in those two frequency bands.

Acknowledgments

The authors thank Maspro Denkoh Corporation for their assistance in the measurements.

References

[1] Recommendation ITU-R BT.2020, "Parameter values for ultra-high definition television systems for production and international programme exchange," Oct. 2015.
[2] Recommendation ITU-R BO.2098, "Transmission system for UHDTV satellite broadcasting," Dec. 2016.
[3] Association of Radio Industries and Businesses, ARIB STD-B44 Ver. 2.0-E1, "Transmission system for advanced wide band digital satellite broadcasting," July 2014.
[4] S. Tanaka, S. Nakazawa, N. Kogou, K. Yamagata, and K. Shogen, "Onboard array-fed reflector antenna for 21-GHz-band direct broadcasting satellite," Proc. 1st European Conference on Antennas and Propagation, Nice, France, Nov. 2006.
[5] S. Nakazawa, M. Nagasaka, M. Kamei, S. Tanaka, and T. Saito, "Prototype 32 elements beam forming network for 21-GHz band broadcasting satellite," Proc. 9th European Conference on Antennas and Propagation, Lisbon, Portugal, April 2015.
[6] M. Kamei, M. Nagasaka, S. Nakazawa, and S. Tanaka, "Development of on-board wideband output filter for 21GHz-band broadcasting satellites," Proc. 21st Ka and Broadband Communications Conference, Ka 14-2, Bologna, Italy, Oct. 2015.
[7] M. Ando, K. Sakurai, and N. Goto, "Characteristics of a radial line slot antenna for 12 GHz band satellite TV reception," IEEE Trans. Antennas Propag., vol.34, no.10, pp.1269–1272, Oct. 1986.
[8] H. Nakano, H. Takeda, Y. Kitamura, H. Mimaki, and J. Yamaguchi, "Low-profile helical array antenna fed from a radial waveguide," IEEE Trans. Antennas Propag., vol.40, no.3, pp.279–284, March 1992.
[9] T. Murata and M. Fujita, "A self-steering planar array antenna for satellite broadcast reception," IEEE Trans. Broadcast., vol.40, no.1, pp.1–6, March 1994.
[10] J. Hirokawa, M. Ando, N. Goto, N. Takahashi, T. Ojima, and M. Uematsu, "A single-layer slotted leaky waveguide array antenna for mobile reception of direct broadcast from satellite," IEEE Trans. Veh. Technol., vol.44, no.4, pp.749–755, Nov. 1999.
[11] M. Takahashi, M. Ando, N. Goto, Y. Numano, M. Suzuki, Y. Okazaki, and T. Yoshimoto, "Dual circularly polarized radial line slot antennas," IEEE Trans. Antennas Propag., vol.43, no.8, pp.874–876, Aug. 1995.
[12] Y. Zhang, Y. Liu, Y. Jiang, W. Hou, and X. Lv, "Design of an X-band dual circularly polarized offset reflector antenna," Proc. IET International Radar Conference 2015, Hangzhou, China, 1465, Oct. 2015.
[13] I. Kim, J.M. Kovitz, and Y. Rahmat-Samii, "Sigmoid profiled septum: Evaluation of the parabolic reflector with the septum feed horn," Proc. 2013 IEEE International Symposium on Antennas and Propagation, 124.4, pp.236–237, Orlando, the United States, July 2013.
[14] M.J. Franco, "High-performance dual-mode feed horn for parabolic

reflectors with a stepped-septum polarizer in a circular waveguide [Antenna designer's notebook]," IEEE Antennas Propag. Mag., vol.53, no.3, pp.142–146, June 2011.
[15] R. Deng, S. Xu, F. Yang, and M. Li, "An FSS-backed Ku/Ka quad-band reflectarray antenna for satellite communications," IEEE Trans. Antennas Propag., vol.66, no.8, pp.4353–4358, Aug. 2018.
[16] D.M. Pozar and S.M. Duffy, "A dual-band circularly polarized aperture-coupled stacked microstrip antenna for global positioning satellite," IEEE Trans. Antennas Propag., vol.45, no.11, pp.1618–1625, Nov. 1997.
[17] F. Ferrero, C. Luxey, G. Jacquemod, and R. Staraj, "Dual-band circularly polarized microstrip antenna for satellite applications," IEEE Antennas Wireless Propag. Lett., vol.4, pp.13–15, June 2005.
[18] K. Yang and K. Wong, "Dual-band circularly-polarized square microstrip antenna," IEEE Trans. Antennas Propag., vol.49, no.3, pp.337–382, March 2001.
[19] M. Nagasaka, S. Nakazawa, and S. Tanaka, "Study on 12/21-GHz dual-circularly polarized receiving antenna for satellite broadcasting," Proc. 2018 IEEE International Symposium on Antennas and Propagation, MO-A1.5P.3, pp.339–340, Boston, the United States, July 2018.
[20] M. Nagasaka, M. Kojima, S. Nakazawa, and S. Tanaka, "Prototype of 12/21GHz-band dual-circularly polarized receiving antenna for satellite broadcasting," Proc. 2018 Asia-Pacific Microwave Conference, FR2-B1-1, Kyoto, Japan, Nov. 2018.
[21] M. Nagasaka, S. Nakazawa, and S. Tanaka, "Dual-circularly polarized offset parabolic reflector antenna with microstrip antenna array for 12-GHz band satellite broadcasting reception," IEICE Trans. Commun., vol.E101-B, no.2, pp.340–348, Feb. 2018.
[22] T. Hori and K. Kagoshima, "Design of Dual-frequency reflector antenna illuminated by a horn and printed antenna array," IEICE Trans. Commun. (Japanese Edition), vol.J76-B2, no.6, pp.504–511, June 1993.
[23] T. Teshirogi, M. Tanaka, and W. Chujo, "Wideband circularly polarized array antenna with sequential rotations and phase shifts of elements," Proc. 1985 International Symposium on Antennas and Propagation, Kyoto, Japan, 1B3-2, pp.117–120, Aug. 1985.
[24] Recommendation ITU-R BO.1213, "Reference receiving earth station antenna pattern for the broadcasting-satellite service in the 11.7–12.75 GHz band," Nov. 2005.
[25] N.A. Adatia, and A.W. Rudge, "Beam squint in circularly polarised offset-reflector antennas," IET Electron. Lett., vol.11, no.21, pp.513–515, Oct. 1975.
[26] T. Hori, "Broadband/multiband printed antennas," IEICE Trans. Commun., vol.E88-B, no.5, pp.1809–1817, May 2005.
[27] CST MICROWAVE STUDIO. Available: http://www.cst.com
[28] W.L. Stutzman and G.A. Thiele, "Gain calculations for reflector antennas," in Antenna Theory and Design, pp.433–436, John Wiley & Sons, New Jersey, 1981.
[29] TICRA GRASP. Available: http://www.ticra.com/
[30] T.A. Milligan, "Random phase errors," in Modern Antenna Design, 2nd ed., pp.393–396, IEEE Press: John Wiley & Sons, New Jersey, 2005.
[31] M. Nagasaka, S. Nakazawa, and S. Tanaka, "Prototype of dual-polarization antenna for satellite broadcasting reception," ITE Technical Report, BCT2014-64, July 2014 (in Japanese).
[32] M. Nagasaka, S. Nakazawa, and S. Tanaka, "12/21 GHz dual-band feed antenna for satellite broadcasting receiving reflector antenna," Proc. 2012 International Symposium on Antennas and Propagation, 3B1-1, pp.790–793, Nagoya, Japan, Nov. 2012.
[33] M. Nagasaka, A. Iwasaki, S. Nakazawa, and S. Tanaka, "Development of advanced receiving antennas for satellite broadcasting," Proc. 12th European Conference on Antennas and Propagation, CS01.5, London, the United Kingdom, April 2018.
[34] NSI-MI Technologies. Available: https://www.nsi-mi.com/
[35] Recommendation ITU-R BO.1900, "Reference receive earth station antenna pattern for the broadcasting-satellite service in the band 21.4–22 GHz in Regions 1 and 3," Jan. 2012.
[36] B-SAT. Available: http://www.b-sat.co.jp/english/
[37] SKY Perfect JSAT Corp. Available: https://www.jsat.net/en/
[38] Y. Suzuki, H. Sujikai, Y. Koizumi, M. Nagasaka, M. Kojima, A. Iwasaki, S. Tanaka, S. Nakazawa, and O. Yamazaki, "Prompt report on wide-band transmission experiment with 21-GHz band broadcasting satellite in NHK STRL OPEN HOUSE 2018," IEICE Technical Report, SAT2018-14, July 2018 (in Japanese).
[39] Association of Radio Industries and Businesses, ARIB STD-B63 Ver. 1.6-E1, "Receiver for advanced wide band digital satellite broadcasting," Dec. 2016.
[40] Y. Suzuki, Y. Matsusaki, M. Kamei, A. Hashimoto, T. Kimura, S. Tanaka, and T. Ikeda, "BCH and LDPC coded wide-band modem for 21-GHz band satellite broadcasting system," 2015 IEEE Radio and Wireless Symposium, MO1D-2, pp.4–6, San Diego, the United States, Jan. 2015.

Masafumi Nagasaka received his B.E. and M.E. degrees in electrical and electronic engineering from Tokyo Institute of Technology, Tokyo, Japan, in 2001 and 2003, respectively. He joined Japan Broadcasting Corporation (NHK) in 2003. Since 2008, he has been engaged in research on antennas for Ku- and Ka-band satellite broadcasting systems at NHK Science & Technology Research Laboratories. He is currently a senior manager of the Planning & Coordination Division of the laboratories. He received the Young Researcher's Award of IEICE in 2011 and the Best Research Presentation Award of ITE in 2014. He is a member of ITE.

Masaaki Kojima received his B.E., M.E., and Ph.D. degrees in electrical and electronic engineering from Tokushima University, Tokushima, Japan, in 2000, 2002, and 2015, respectively. He joined Japan Broadcasting Corporation (NHK) in 2002. Since 2006, he has been engaged in research on the nonlinear characteristics of broadcasting satellite transponders at NHK Science & Technology Research Laboratories. He is currently a principal research engineer of the laboratories. He received the IEEE CASS Shikoku Chapter Best Paper Award in 2015 and the JC-SAT Award from IEICE in 2017. He is a member of ITE and IEEE.

Hisashi Sujikai received his B.E. and M.E. degrees in electrical and electronic engineering from Waseda University, Tokyo, Japan, in 1991 and 1993, respectively. From 2013 to 2017, he was a senior manager of the Engineering Administration Department of Japan Broadcasting Corporation (NHK). Since 2017, he has been engaged in research on future satellite broadcasting systems at NHK Science & Technology Research Laboratories. He is currently a senior research engineer of the laboratories. He is a vice chair of the Technical Committee on Satellite Telecommunications of IEICE and a member of ITE.

Jiro Hirokawa received the B.S., M.S. and D.E. degrees in electrical and electronic engineering from Tokyo Institute of Technology (Tokyo Tech), Tokyo, Japan in 1988, 1990 and 1994, respectively. He was a Research Associate from 1990 to 1996 and an Associate Professor from 1996 to 2015 at Tokyo Tech. He is currently a Professor there. He was with the antenna group of Chalmers University of Technology, Gothenburg, Sweden, as a Postdoctoral Fellow from 1994 to 1995. His research area has been in slotted waveguide array antennas and millimeter-wave antennas. He received IEEE AP-S Tokyo Chapter Young Engineer Award in 1991, Young Engineer Award from IEICE in 1996, Tokyo Tech Award for Challenging Research in 2003, Young Scientists' Prize from the Minister of Education, Cultures, Sports, Science and Technology in Japan in 2005, Best Paper Award in 2007 and a Best Letter Award in 2009 from IEICE Communications Society, and IEICE Best Paper Award in 2016 and 2018. He is a Fellow of IEEE.